Biochimica et Biophysica Acta 1797 (2010) 1736–1748

Contents lists available at ScienceDirect

Biochimica et Biophysica Acta

journal homepage: www.elsevier.com/locate/bbabio

3-D modelling of chloroplast structure under (Mg^{2+}) magnesium ion treatment. Relationship between thylakoid membrane arrangement and stacking

Izabela Rumak [a,b], Katarzyna Gieczewska [a,b], Borys Kierdaszuk [c], Wiesław I. Gruszecki [d], Agnieszka Mostowska [b], Radosław Mazur [a], Maciej Garstka [a,*]

[a] Department of Metabolic Regulation, Institute of Biochemistry, Faculty of Biology, University of Warsaw, Miecznikowa 1, PL-02-096 Warsaw, Poland
[b] Department of Plant Anatomy and Cytology, Institute of Experimental Plant Biology, Faculty of Biology, University of Warsaw, Miecznikowa 1, PL-02-096 Warsaw, Poland
[c] Department of Biophysics, Institute of Experimental Physics, Faculty of Physics, University of Warsaw, Zwirki i Wigury 93, PL-02-089 Warsaw, Poland
[d] Department of Biophysics, Institute of Physics, Maria Curie-Sklodowska University, Maria Curie-Sklodowska sq. 1, PL-20-031 Lublin, Poland

ARTICLE INFO

Article history:
Received 2 March 2010
Received in revised form 11 May 2010
Accepted 6 July 2010
Available online 16 July 2010

Keywords:
3-D models
Chloroplast structure
Stacking
Magnesium ions
CLSM
FTIR

ABSTRACT

We performed for the first time three-dimensional (3D) modelling of the entire chloroplast structure. Stacks of optical slices obtained by confocal laser scanning microscope (CLSM) provided a basis for construction of 3D images of individual chloroplasts. We selected pea (*Pisum sativum*) and bean (*Phaseolus vulgaris*) chloroplasts since we found that they differ in thylakoid organization. Pea chloroplasts contain large distinctly separated appressed domains while less distinguished appressed regions are present in bean chloroplasts. Different magnesium ion treatments were used to study thylakoid membrane stacking and arrangement. In pea chloroplasts, as demonstrated by 3D modelling, the increase of magnesium ion concentration changed the degree of membrane appression from wrinkled continuous surface to many distinguished stacked areas and significant increase of the inter-grana area. On the other hand 3D models of bean chloroplasts exhibited similar but less pronounced tendencies towards formation of appressed regions. Additionally, we studied arrangements of thylakoid membranes and chlorophyll–protein complexes by various spectroscopic methods, Fourier-transform infrared spectroscopy (FTIR) among others. Based on microscopic and spectroscopic data we suggested that the range of chloroplast structure alterations under magnesium ions treatment is a consequence of the arrangement of supercomplexes. Moreover, we showed that stacking processes always affect the structural changes of chloroplast as a whole.

1. Introduction

Photosynthetic light-driven reactions in higher plants take place in chlorophyll–protein complexes (CP)—photosystems I and II (PSI/II) associated with respective antennae (LHCI/II). These complexes are localized inside the thylakoid membranes that are structurally differentiated into stacked (appressed) multilamellar regions (grana) and unstacked (non-appressed) stroma thylakoid interconnecting grana. Such thylakoid membrane arrangement creates three dimensional (3D) network that encloses single compartment inside it [1]. Spatial thylakoid organization is related to segregation of main CP complexes organized hierarchically in supercomplexes and megacomplexes [1,2]. LHCII–PSII supercomplex, named as photosynthetic unit PSIIα, comprises dimer of PSII core, minor light-harvesting complexes (Lhcb4–6) and variable amounts of LHCII trimers (Lhcb1–3) [1,3] and occurs exclusively in grana regions [4,5]. The monomeric PSI core complex with four LHCI subunits (Lhca1–4) [6] and with temporarily bound LHCII complex [7] forms LHCI–PSI supercomplexes localized in unstacked thylakoid regions [4,5]. Furthermore, ATP-synthase as well as monomeric PSII (PSIIβ) without LHCII trimers are found in the stroma thylakoids [1,4]. Such membrane structure is highly dynamic as a result of CP supercomplex rearrangement in response to environmental factors, e.g., under variable light conditions [8] and other abiotic stresses [9,10].

Over the last decade 3D models of thylakoids organization inside chloroplasts have been discussed. The first model suggests that grana are formed by folding of a single continuous membrane [11]. The second one assumes the existence of cylindrical grana discs piled one on top of the other and connected to each other with right-handed helices of stroma thylakoids [12]. The grana discs are connected to each other by stroma thylakoids helices, that makes multiple contacts. Grana are formed by symmetrical invagination of stroma thylakoid pairs into piles of three discs [13]. The last model assumes dynamic changes in molecular structure of membrane bilayer. Granum stack is formed by bifurcation of stroma lamellae and subsequent fusion of newly created membranes. Edges of adjacent membranes bend and fuse with neighboring lamellae forming thylakoid stacks [14].

Abbreviations: Chl, chlorophyll; CLSM, confocal laser scanning microscopy; CP, Chlorophyll–protein; Em, emission wavelength; Ex, excitation wavelength; FTIR, Fourier-transform infrared spectroscopy; RLS, resonance light scattering

* Corresponding author. Tel.: +48 22 5543215; fax: +48 22 5543221.
E-mail address: garstka@biol.uw.edu.pl (M. Garstka).

0005-2728/$ – see front matter © 2010 Elsevier B.V. All rights reserved.
doi:10.1016/j.bbabio.2010.07.001

Complete model of a 3D network of thylakoid membrane structure is still under discussion [13,15].

Formation of appressed regions depends on two connected processes: (i) surface interaction between adjacent membranes in grana stacks [16] and (ii) protein movement in lateral plane of thylakoids [17,18]. Spontaneous appression of thylakoid membranes is a consequence of van der Waals attraction and thermodynamic tendency to increase the overall entropy within chloroplast stroma. On the contrary, unstacking of grana is induced by electrostatic and hydratation repulsion between membranes [16]. Charge mismatch of photosystems and size difference between PSII and PSI are the main factor determining lateral separations of CP complexes in stacked thylakoids [5,17,19]. The structure of grana stacks is mainly stabilized by ordered arrangement of LHCII–PSII and LHCII complexes [1], while the unstacking of grana causes unbinding of LHCII from supercomplexes and random distribution of photosystems in the lateral plane of the thylakoid membrane [20,21].

In vitro unstacking of thylakoid membranes was observed in low-ionic-strength buffers, whereas addition of cations, especially Mg^{2+} ions, resulted in spontaneous grana formation, due to enhanced electrostatic screening of thylakoid membranes surface charge [16 and references therein]. This commonly known phenomenon was investigated mainly on the level of thylakoid membranes by different spectroscopic methods [22,23] as well as by transmission [16] and freeze-fracture electron microscopy [21] and atomic-force microscopy [24]. However, there is not much data concerning the effect of Mg^{2+} ions on the overall chloroplast structure [16].

The aim of the present study is to scrutinize the Mg^{2+}-induced lateral and vertical arrangement of thylakoid membranes and changes of the overall chloroplast structure visualized by confocal laser scanning microscopy (CLSM). Since recent data suggest that the stacking process strictly depends on the arrangement of CP complexes [21], we used different magnesium treatments as a tool to study thylakoid membrane stacking and arrangement in chloroplasts isolated from pea and bean plants. These plant species under investigation differ in the structural thylakoid membrane organization [9,10,25]. Spectroscopic methods like low-temperature fluorescence, resonance light scattering (RLS) and Fourier-transform infrared spectroscopy (FTIR) enabled appraising quantitative and qualitative arrangement of the thylakoid membranes under the stacking process. CLSM image analysis allowed to visualize the Mg^{2+}-induced changes in the entire chloroplast structure and to make three-dimensional (3D) organelle models. Relations between biophysical and microscopic data are discussed in details. Moreover for the first time the FTIR and 3D visualization of CLSM images were adapted to investigation of grana stacking.

2. Materials and methods

2.1. Plant materials and growth conditions

Pea (*Pisum sativum* L. *cv*. Demon) and bean (*Phaseolus vulgaris* L. *cv*. Eureka) plants (both from PlantiCo Zielonki, 05-082 Babice Stare, Poland) were grown in 3 L perlite-containing pots in a climated room (22 °C/20 °C day/night temperature) at a photosynthetic active radiation (PAR) of 200 μmol photons m^{-2} s^{-1} during a 16-h photoperiod and relative humidity of 60–70%. Plants were fertilized with full Knop's nutrient solution. Fully expanded leaves of 18- and 14-day-old pea and bean, respectively, were harvested 30 min after light was on.

2.2. Preparation of thylakoid membranes and intact chloroplasts

Chloroplasts were isolated by homogenization of pea and bean leaves in a buffer A (20 mM Tricine-NaOH, pH 7.5) containing 330 mM sorbitol, 15 mM NaCl, 4 mM $MgCl_2$ and 40 mM ascorbate. The homogenate was filtered and centrifuged at 2000*g* for 5 min to obtain chloroplasts pellet. Subsequently buffer B (20 mM Tricine-NaOH pH 7.0) containing 15 mM NaCl and 4 mM $MgCl_2$ was used for preparation of the thylakoid membranes from chloroplasts. After centrifugation at 6000*g* for 10 min pellet was resuspended in a buffer C (20 mM HEPES-NaOH pH 7.0) containing 330 mM sorbitol, 15 mM NaCl, 4 mM $MgCl_2$. Probes were centrifuged at 6000*g* for 10 min and after that thylakoid membranes were resuspended in small amount of buffer C. Thylakoid membranes were always freshly prepared before each experiment and were kept on ice and in dark for subsequent use. Intact chloroplasts were isolated in semi-frozen buffer A by gentle homogenization of pea and bean leaves. After filtration the intact chloroplasts were centrifuged at 2000*g* for 3 min. Pellet obtained in a such way was very gently resuspended in a small amount of buffer C and immediately used for confocal laser scanning microscopy (CLSM) investigation. The integrity of at least 80% chloroplasts was determined by ferricyanide reduction before and after osmotic shock [26]. Moreover, chloroplasts with a damaged envelope were not a subject of the CLSM analysis. The concentration of chlorophyll (Chl) was quantified spectrophotometrically after extraction with 80% acetone [26].

2.3. $MgCl_2$ dependent thylakoid stacking

Thylakoid preparation was diluted to appropriate Chl concentration (see figure legends) by addition of small volume of suspension (4–10 μl) to 4 ml of 20 mM HEPES-NaOH (pH 7.5) buffer containing 330 mM sorbitol and appropriate concentration of $MgCl_2$ (0–6 mM). Spectra of the samples were examined after 10 min incubation in dark at the saturated point of fluorescence emission for the appropriate $MgCl_2$ concentration.

2.4. Measurements of thylakoid fluorescence

Steady-state fluorescence emission spectra at 25 °C (298 K) were determined with the help of Shimadzu RF-5301PC spectrofluorimeter with 3- and 10-nm spectral resolution for excitation and emission. Samples were placed in quartz cuvette (10-mm optical path length) and magnetically stirred to prevent settling. Fluorescence spectrum (600–800 nm) was recorded 3 times. First scan was carried out to eliminate light-dependent changes in fluorescence intensities, which did not exceeded 2%. The second and the third scans were used to obtain an average fluorescence spectrum of the sample. Steady-state fluorescence spectra at 120 K were monitored with a Spex FluoroMax spectrofluorimeter with 2-nm spectral resolution for excitation and emission. Samples were thermostated using a home-made liquid nitrogen cryostat (Institute of Physics, Polish Academy of Sciences, Warsaw). Temperature was measured directly in the glassy solution by a diode thermometer, with an accuracy of 0.5 K. After dark-incubation thylakoid samples were resuspended in 2 ml of 20 mM HEPES-NaOH buffer (pH 7.5) containing appropriate concentration of $MgCl_2$ and 80% (v/v) glycerol in 10×10 mm polymethacrylate cuvettes (Sigma, USA). The total optical density of the thylakoid samples did not exceed 0.1 to minimize inner-filter effects. Low temperature measurements were performed at 120 K, since temperature stability below 120 K was not sufficient, especially near boiling temperature of liquid nitrogen.

The decomposition of fluorescence spectra was performed by using Grams/AI 8.0 Spectroscopy Software (Thermo Electron Corporation, USA) programs with 5 Gaussian subbands. The parameters of the components were based on data of [27]. The bands with maxima at 680, 690, 696, 730 and 755 nm were ascribed to LHCII (trimers, monomers), RC PSII complex, LHCII (aggregated trimers), core complex and LHC of PSI [27 and references therein], respectively.

2.5. Absorbance and resonance light scattering (RLS) measurements

Room temperature RLS spectra were recorded in a synchronous mode at 90° with respect to the incident light, using a Shimadzu RF-5301PC spectrofluorimeter. The excitation and emission bandwidths were set to 1.5 nm. Each spectrum was recorded 3 times. After RLS measurements the same probe was used to achieve absorption spectra using a Cary 50 Bio spectrophotometer in quartz cuvette; each spectrum was recorded 2 times.

2.6. Fourier-transform infrared spectroscopy (FTIR) measurements

Thylakoid membranes suspension was resuspended in a D_2O-based 20 mM Hepes–NaOH (pH 7.0) buffer containing 330 mM sorbitol and appropriate $MgCl_2$ concentration (0 or 6 mM) and then centrifuged at 7200*g* for 10 min at 4 °C. This step was repeated three times to replace H_2O based buffers with D_2O ones. Fourier-transform infrared (FTIR) spectra were recorded with a Bruker Vector 33 spectrometer equipped with a horizontal attenuated total reflection (ATR) cell. Sample containing liquid thylakoids was deposited on a ZnSe crystal and spectra were recorded in darkness in argon atmosphere with 0.6 cm^{-1} spectral resolution. The buffer without membranes was used as a control. For each background and for each sample spectrum 25 interferograms were averaged and Fourier transformed. Data analysis was carried out with Grams/AI 8.0 Spectroscopy Software (Thermo Electron Corporation, USA). Before the data analysis a linear baseline was subtracted in the three ranges: 1710–1585 cm^{-1} corresponding to C=O stretching vibration region of polypeptide chains (Amide I region), 1790–1590 cm^{-1} and 3000–2800 cm^{-1}, corresponding to the deformation and to the stretching vibrations of CH_2 and CH_3 groups of membrane lipids acyl chains, respectively. The Amide I region of the spectrum was fitted with five Gaussian component bands, the 3000–2800 cm^{-1} region was fitted with both Gaussian and Gaussian–Lorentzian component bands. The fit of all parameters (frequency, bandwidth, etc.) was based on [28]. The accuracy of the component band frequency determination was better than 0.1 cm^{-1}.

2.7. Transmission electron microscopy (TEM)

Samples of pea and bean leaves were taken for TEM as described in [10]. Pieces of about 1–4 mm^2 in area were cut from middle part of leaf. The material was fixed in 2.5% glutaraldehyde in 50 mM cacodylate buffer at pH 7.4 for 2 h, washed in buffer and placed in 2% OsO_4 at 4 °C in 50 mM cacodylate buffer for about 12 h. The specimens, dehydrated in a graded acetone series, were embedded in a low viscosity epoxy resin and cut on a Leica UCT ultramicrotome. Sections stained with uranyl acetate and lead citrate were examined with a JEM 1200EX electron microscope with 26000× magnification.

2.8. Confocal laser scanning microscopy (CLSM) and 3D reconstruction

Isolated intact chloroplasts (30 μg Chl ml^{-1}) were suspended in 20 mM HEPES-NaOH (pH 7.5) containing 330 mM sorbitol, 6% (v/v) glycerol, 30 μM DCMU and $MgCl_2$ in appropriate concentration (0–6 mM). After 10 min on ice and dark incubation suspension was placed on a poly-L-lysine layer (1 mg ml^{-1}) and immobilized on a microscopic glass. Samples were imaged using Zeiss LSM 510 confocal laser scanning fluorescence microscope equipped with a PlanApo 63×, NA 1.4 objective lens. Excitation was performed at 543 nm output from a helium-neon laser. Fluorescence emission was collected through a 560 nm long pass filter, while confocal aperture was set at 106 μm (1 airy unit). Z-series (79–104 optical slices) of 1024×1024 pixels and 8 bit images were collected and those which were not affected by fluorescence quenching due to the light-exposure in microscope were taken to computer analysis. To improve signal-to-noise ratio data stacks were deconvolved using the Huygens Suite 2.8 software (Scientific Volume Imaging, The Netherlands). Three-dimensional models of chloroplasts were created by KS 400 (Zeiss) software by voxels rendering in the gradient mode.

3. Results

3.1. Distribution of Chl fluorescence inside chloroplasts in isoosmotic medium

Visualization of Chl fluorescence by CLSM enabled observation *in situ* of thylakoid membranes inside intact chloroplasts. Fluorescent discrete red spots separated from each other by dark space inside each chloroplast revealed by CLSM were seen in both species. These bright red, regular spots were attributed mainly to appressed thylakoid membranes containing LHCII–PSII supercomplexes and LHCII trimers rather than to non-appressed thylakoids containing PSI, because PSI fluorescence at 25 °C was rather weak [29]. Size and shape of fluorescent red spots, corresponding to grana stacks, differ between species. For example *Pisum* chloroplasts, approximately of 3–4 μm in diameter had brightly red fluorescent areas of dimensions of about 500 nm, whereas *Spathiphyllum* chloroplasts were bigger and had fluorescent discs of dimensions of about 0.8–1 μm [29]. Our experiments with intact chloroplast isolated from leaves of pea (*Pisum sativum*) and bean (*Phaseolus vulgaris*), and both incubated in isoosmotic medium containing 15 mM NaCl and 4 mM $MgCl_2$ (buffer C), revealed that bigger and better distinguished fluorescent discs were observed in pea than in bean chloroplasts (Fig. 1A, B). Our observations of chloroplasts by CLSM are consistent with transmission electron microscopy (TEM) images of pea and bean chloroplasts of leaf mesophyll. TEM images of pea showed large appressed thylakoid regions, clearly separated from each other by non-appressed ones and oriented in parallel plane (Fig. 1C). On the other hand bean chloroplasts contained numerous non-appressed thylakoid regions with some appressed ones irregularly distributed within chloroplasts (Fig. 1D). These TEM images of thylakoid arrangement in bean chloroplasts were a counterpart of smaller and less distinguished fluorescent areas corresponding to the appressed regions. Chloroplast images from intact chloroplasts revealed by CLSM and from leaf tissue *in situ* revealed by TEM were consistent with each other and give similar information on the different distribution of appressed and non-appressed thylakoids in bean and pea chloroplasts. This observation suggested different arrangement of LHCII/PSII rich grana membranes inside chloroplast of both species. CLSM and TEM results were confirmed by steady-state fluorescence emission spectra at 120 K, a useful method for investigation of CP complexes arrangement [9,10]. For isolated thylakoids incubated in buffer C, excited at 470 nm the ratio of main fluorescence bands (735 nm and 680 nm) was 0.91 and 1.3 for pea and bean respectively. We suggested that the excitation energy transfer from external antenna to PSII versus PSI core was more effective in pea than bean thylakoid [25], probably due to diverse arrangement of CP super- and megacomplexes, as was previously shown by mild-denaturing electrophoresis [9,10]. It has been observed that the degree of thylakoid membrane stacking is correlated with Chl *a*/Chl *b* ratio due to different ratio of antenna to core complexes [30]. However in our case of pea and bean thylakoids this parameter has the same value, estimated to about 3.0 [9,10] suggesting different proportion between antenna (LHCII/LHCI) and core (PSII/PSI) complexes in these two species. Therefore, pea chloroplasts with large appressed areas and bean chloroplasts with poorly distinguished appressed regions (Fig. 1) were perfect models to study the effect of Mg^{2+} ions on the overall chloroplast structure.

3.2. Effect of $MgCl_2$ concentration on chlorophyll fluorescence yield and relative contribution of CP complexes to fluorescence spectra of isolated thylakoid membranes

Changes in steady-state fluorescence emission intensity, at 680 nm at room temperature, were directly related to arrangements of LHCII/

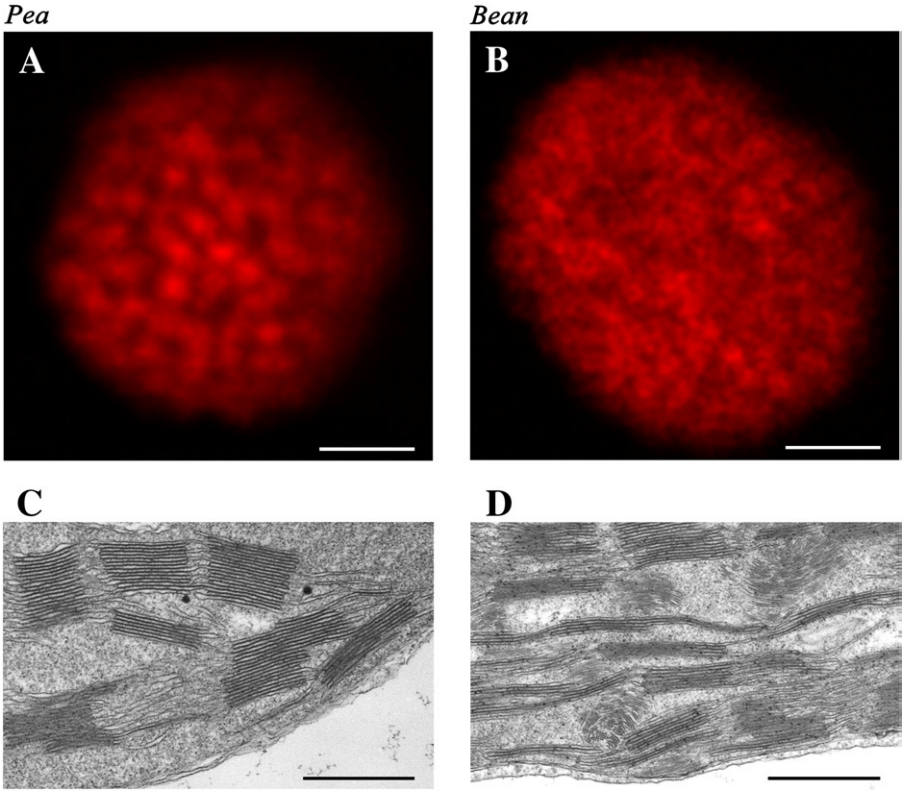

Fig. 1. Differences between pea and bean chloroplasts revealed by CLSM (A, B) and TEM microscopy (C, D). For CLSM investigation the intact chloroplasts were incubated in isoosmotic medium containing 15 mM NaCl and 4 mM $MgCl_2$. Each image presents the middle cross-section of deconvolved stack of CLSM images. White bar = 2 μm. Images are representative for at least 20 independent experiments. TEM image represents the thylakoid arrangements in leaf chloroplast. Dark bar = 500 nm.

PSII complexes inside the thylakoid membranes [22], therefore the effect of different Mg^{2+} ion concentrations, in the range 0–6 mM $MgCl_2$, on Chl fluorescence emission intensity was investigated in isolated thylakoids (Fig. 2A, B). In pea thylakoids Chl fluorescence increased at low cation concentrations rapidly and linearly up to 1 mM and was constant up to 6 mM $MgCl_2$ (Fig. 2A). In bean thylakoids Chl fluorescence increased slowly and reached saturation at 4 mM $MgCl_2$ (Fig. 2A). However, the final increase of Chl fluorescence in bean was six times lower than in pea thylakoids, indicating less dynamic rearrangements of LHCII/PSII complexes in bean than in pea thylakoids.

Detailed analysis of CP complexes arrangements under conversion from unstacking to stacking conditions was performed by low temperature fluorescence at 120 K. Fluorescence was only slightly different from that measured at 77 K [31], and enabled analysis of the relative contribution of individual CP complexes to the overall Chl fluorescence in thylakoid membranes [9,10,27]. Low-temperature emission spectra displayed two prominent Gaussian components at 680 and around 735 nm (Fig. 3), presenting the sum of fluorescence emitted from LHCII/PSII (PSIIα) and LHCI/PSI complexes [6,27], respectively.

In pea thylakoids incubated without Mg^{2+} ions and excited at 412 (Chl *a*) or 470 nm (Chl *b*) (Fig. 3A, C), the ratio of areas beneath respective bands (PSI/PSII) were estimated to 3.06 and 2.68. Thus, under destacking conditions relative emission from Chl species associated with PSI/LHCI complexes was larger than PSII/LHCII fluorescence. Incubation of pea thylakoids with 6 mM $MgCl_2$ caused significant decrease of the PSI/PSII fluorescence ratio (Fig. 3B, D), suggesting rearrangement between CP complexes. Moreover, stronger $MgCl_2$ effect in samples where Chl fluorescence was

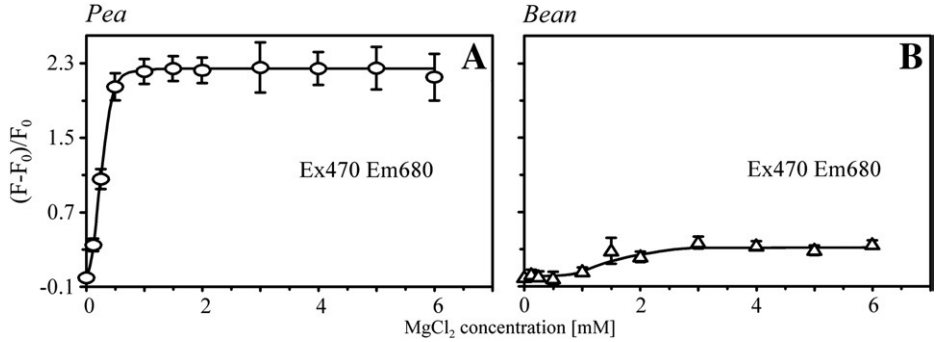

Fig. 2. Effect of $MgCl_2$ concentration on the relative changes of steady-state fluorescence emission intensity (Ex 470 nm) at 25 °C in thylakoid membranes (6 μg Chl ml^{-1}) isolated from pea (A) (empty circles) and bean (B) (empty triangles) leaves. F_0 value is the maximum of fluorescence (at about 680 nm) of thylakoid membranes incubated without Mg^{2+} ions (0 mM $MgCl_2$). *F* values were estimated as a maximum of steady-state fluorescence emission spectra of thylakoid membranes at increasing $MgCl_2$ concentration. The data are mean values ± SD from 3 independent experiments.

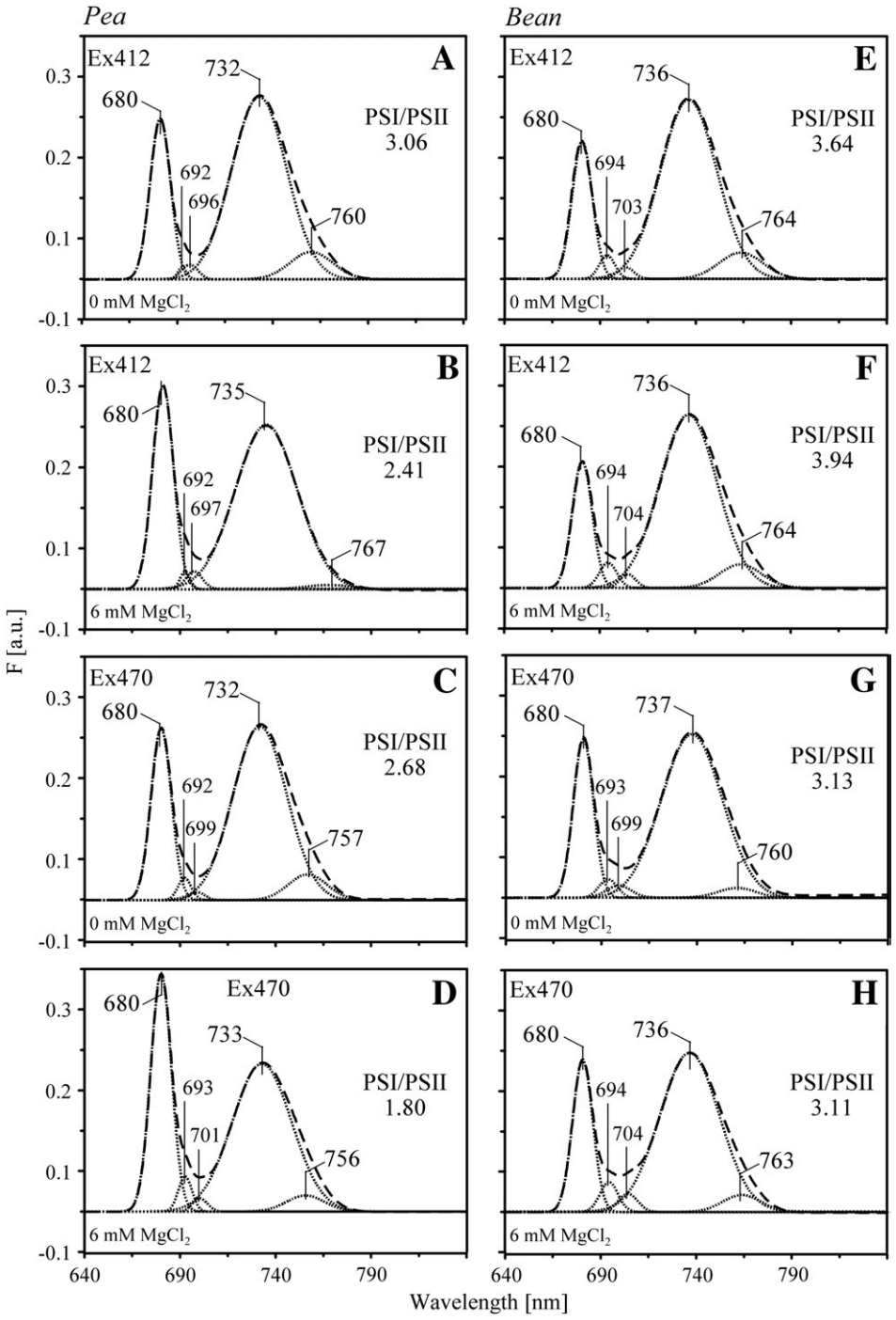

Fig. 3. Effect of $MgCl_2$ concentration on fluorescence emission spectra of isolated thylakoids (3 μg Chl ml^{-1}) at 120 K. Fluorescence emission spectra of thylakoids isolated from pea (A–D) and bean (E–H) leaves incubated without $MgCl_2$ (0 mM concentration) (A, C and E, G) or in the presence of 6 mM $MgCl_2$ (B, D and F, H). Spectra were excited at 412 (A, B, E, F) or 470 nm (C, D, G, H), respectively. Spectra were normalized to the area of 100 under the spectrum and subsequently deconvolved into Gaussian bands as described in Materials and methods. Dashed line–fitted spectra, dotted lines–Gaussian components. The presented spectra are representative for three independent experiments.

induced by Chl *b* excitation, rather than in thylakoids excited at Chl *a* specific band, suggests an increase in connectivity between external antennae and core complexes of PSII [22]. Furthermore, the increase of PIIα with simultaneous decrease of PSI fluorescence intensity might also indicate certain energy spillover from PSI to PSII [32]. In pea thylakoids under $MgCl_2$ treatment, the minor Gaussian components around 699 nm, attributed to LHCII multi-aggregates disconnected from PSII [9,27,33], were practically unchanged (Fig. 3A–D), suggesting that stacking process did not induce aggregation of external antennae outside PSIIα complexes.

Gaussian deconvolution of low-temperature Chl fluorescence spectra of bean thylakoids revealed that $MgCl_2$ treatment did not induce large changes in relative contribution of LHCII/PSII and LHCI/PSI to overall fluorescence (Fig. 3E–H). In samples excited at 412 (Chl *a*) unexpected slight increase of the PSI/PSII fluorescence ratio was observed (Fig. 3E, F) suggesting certain changes in the arrangements of PSII and/or PSI core complexes. Furthermore, the five nanometer red shift of band related to multiaggregates of LHCII (Fig. 3G, H), might indicate changes in the arrangement of antennae complexes outside PSIIα. However, these data suggest that the energy

distribution in bean thylakoids between PSII/PSI is practically independent on $MgCl_2$ concentration.

3.3. Changes in relative efficiency of light harvesting in thylakoids under stacking process

Fig. 4A and B represents 120 K steady-state fluorescence excitation spectra, centered at 735 nm, recorded in pea and bean thylakoids incubated in the absence (0 mM) or in the presence of Mg^{2+} ions (6 mM). These spectra showed typical excitation in the Soret region due to light-harvesting by Chl *a* (414–435), Chl *b* (472 nm), superimposed bands of carotenoid pigments (around 497 nm), as well as bands in the red wavelengths around 600–700 nm, solely due to excitation of Chl *a* (675–676 nm) and Chl *b* (646 nm) [34]. Calculated difference excitation spectra of pea thylakoids (Fig. 4C) (Em 735 and 680 nm) revealed differences between stacking and unstacking conditions and showed significant negative bands at 423 nm in the Soret region and noticeable positive bands at 510 nm. In scan centered at 735 nm, the additional wide negative band at around 470 nm as well as large positive band at 679 nm in Q region of chlorophyll were present. The decrease and blue-shift of B_x bands of Chl *a* (423 nm), Chl *b* (459 nm), and xanthophylls (481 nm), as well as slight red-shift of Q_y band of Chl *a* (679 nm), suggest a decrease of energy transfer efficiency from Chl *b* antennae complexes to Chl species at 735 nm and a significant alteration of pigment arrangements under stacking process. The difference excitation spectra of bean thylakoids (Fig. 4D) for spectra centered at 680 and 735 showed negative bands at 430 nm. However, insignificant changes for Chl *b* band (462 nm) and minor changes in Q region of chlorophyll were observed. Thus, the decrease and blue-shift of B_x band exclusively for Chl *a* (430 nm) suggest that the $MgCl_2$-induced conformational changes in bean thylakoids might be restricted to the core CP complexes.

3.4. Effect of $MgCl_2$ concentration on relative changes in absorbance and resonance light scattering (RLS) of isolated thylakoid membranes

Steady-state 298 K (25 °C) electronic absorption spectra revealed properties of pigments bound in CP complexes [33]. Therefore the analysis of relative contribution of individual bands in one minus transmission spectra (100-T) was performed for pea and bean thylakoids incubated in solutions with different (0–6 mM) $MgCl_2$ concentrations (Fig. 5A, B). Pea and bean spectra showed similar maxima at 438 and 443 nm (Chl *a*), 472 and 475 nm (Chl *b*) as well as at 681 and 683 nm (Q_y of Chl *a*), respectively, comparable to the fluorescence excitation spectra (cf. Fig. 4). However the ratio of the Soret to the Q band was higher in pea than in bean thylakoids what confirmed different arrangements of CP complexes (cf. Fig. 1). Absorption difference spectra of $MgCl_2$ treated pea thylakoid membranes, relative to that of thylakoids incubated without Mg^{2+} ions (Fig. 5C), exhibited two large and blue-shifted negative bands at 420 and 668 nm. Similarly, absorption difference spectra of bean

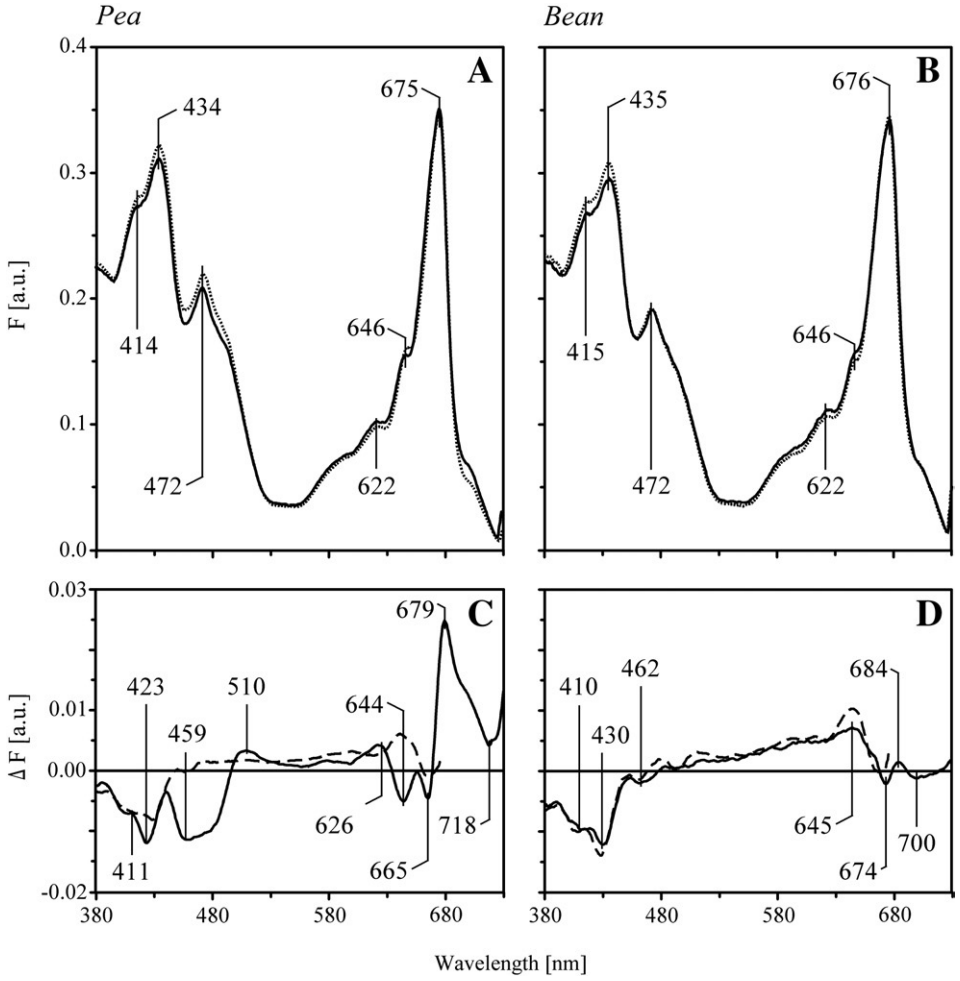

Fig. 4. Effect of $MgCl_2$ concentration on fluorescence excitation spectra (Em 735 nm) of pea (A) and bean (B) thylakoids (3 μg Chl ml^{-1}) at 120 K. Dotted line—spectra recorded in buffer without Mg^{2+} ions, solid line—in buffer with 6 mM $MgCl_2$. Fluorescence excitation difference spectra of thylakoids from pea (C) and bean (D) at 6 mM $MgCl_2$ relative to that at 0 mM $MgCl_2$ were calculated for the respective excitation spectra normalized to the area of 100 under the spectrum. Dashed line–spectra centered at 680 nm, solid line–at 735 nm.

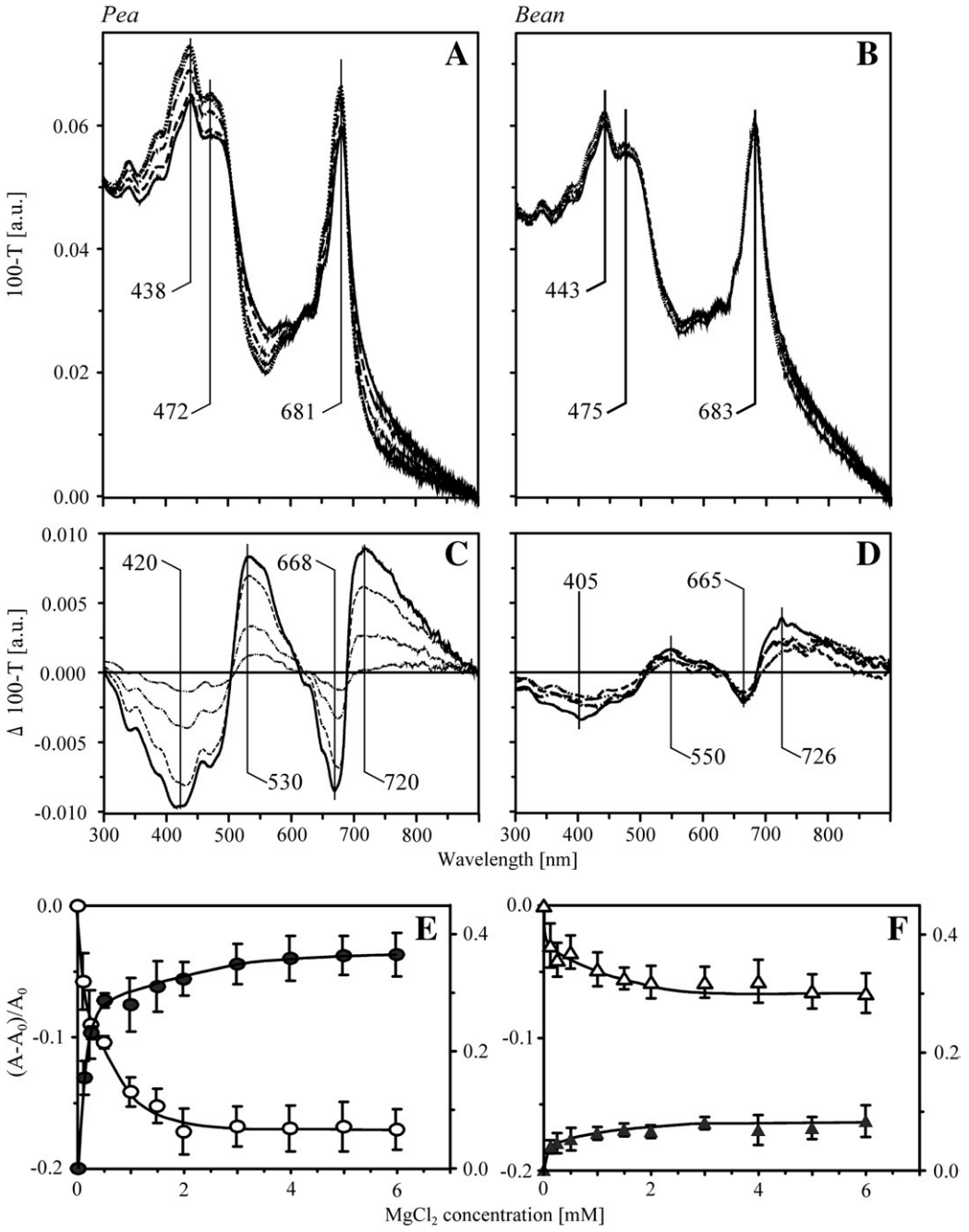

Fig. 5. Effect of $MgCl_2$ concentration on the one minus transmission spectra (100-T) at 25 °C for thylakoids (18 μg Chl ml^{-1}) isolated from pea (A) and bean (B) leaves in absence (dotted line) and in the presence of 0.125 mM (dashed-dotted-dotted), 0.25 mM (dashed-dotted), 0.50 mM (dashed), 6 mM (solid) $MgCl_2$. Spectra were normalized to the area of 100 under the spectrum. Difference spectra for respective samples incubated with elevated $MgCl_2$ minus spectrum for sample without $MgCl_2$ are presented in panel C and D. Spectra are representative for three independent experiments. Panels E and F show effect of $MgCl_2$ concentration at 25 °C on the relative changes of absorption in thylakoid membranes (18 μg Chl ml^{-1}) isolated from pea and bean leaves, respectively. A_0 and A are the absolute absorption values at 440 (closed circles and closed triangles) or 520 nm (empty circles and empty triangles) of thylakoid membranes in the absence and presence of $MgCl_2$ at indicated concentrations. The data are mean values ± SD from 3 independent experiments.

thylakoids (Fig. 5D) revealed negative bands around 405 and 665 nm, but with four-times smaller intensity values.

Notice that the difference excitation spectra (cf. Fig. 4C, D) and difference 100-T spectra (Fig. 5C, D) were different. The observed large positive bands around 530 and 720 nm in pea thylakoids (Fig. 5C), as well as small bands around 550 and 726 nm in bean (Fig. 5D), were related to components of light scattering [33]. In contrast to the Chl fluorescence rise (cf. Fig. 2A) the relative absorption (at 440 and 520 nm) in pea thylakoids reached maximum slightly above 4 mM of $MgCl_2$ concentration (Fig. 5E). In bean thylakoids (Fig. 5F) the course of absorbance was similar but changes were considerably smaller. It was reported that analogous changes in absorbance reflect an increase of pigments interaction, probably due to CP aggregation or thylakoids stacking [22,34–36].

Resonance light scattering (RLS) spectra of both pea and bean thylakoids displayed two distinct maxima at 516 and 692/694 nm (Fig. 6A and B), attributed to the Soret band and the chlorophyll Q band [33], respectively. In comparison with light scattering components in absorbance spectra (Fig. 5C), RLS was a more sensitive and selective indicator of CP aggregation processes [33,37] and of the degree of grana stacking [23]. Presented here RLS spectra of pea thylakoids incubated with gradually increasing $MgCl_2$ concentration (0–6 mM), showed

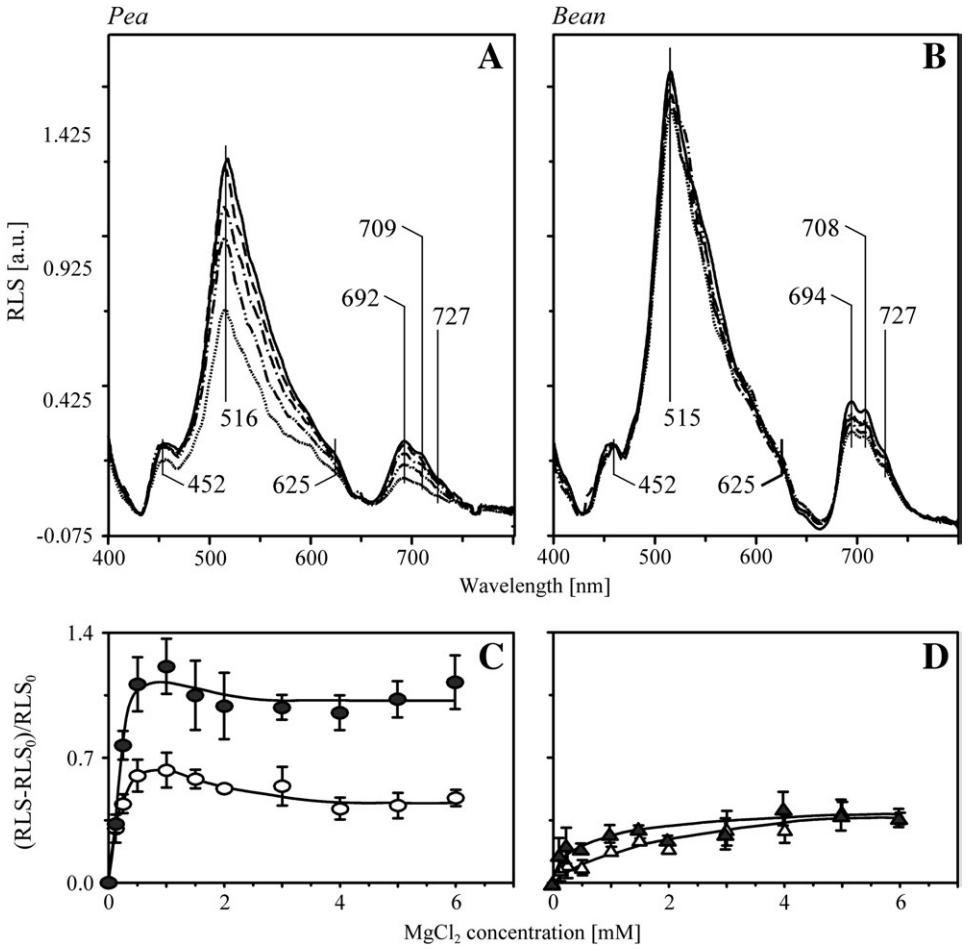

Fig. 6. Resonance light scattering (RLS) spectra recorded at 25 °C from pea (A) and bean (B) thylakoid membranes (18 μg Chl ml^{-1}) incubated without Mg^{2+} ions (dotted line) or elevated $MgCl_2$ concentrations as described in legend to Fig. 5. Spectra are representative for three independent experiments. Panel C and D show the effect of $MgCl_2$ concentration on relative changes of RLS at 515 (closed circles and closed triangles) and 692 nm (empty circles and empty triangles) for pea and bean thylakoids, respectively. The RLS data were withdraw from respective RLS spectra and calculated as described in legend to Fig. 5.

gradual increase of intensities at 516 and 692 nm bands (Fig. 6A), probably due to the presence of stacked structure [23 and references cited therein]. The relative increase of RLS in pea thylakoids was linear at low cation concentrations, reached maximum already at 0.5 mM $MgCl_2$ and slightly decreased with further increase of Mg^{2+} concentration (Fig. 6B). Furthermore, the band shape did not change (Fig. 6A), indicating that $MgCl_2$ induced stacking of pea thylakoids without significant changes in the arrangement of CP complexes [33]. On the contrary, $MgCl_2$ effect on RLS spectra of bean thylakoids was weak (Fig. 6C), and slow RLS rise in bean thylakoids (Fig. 6D) was similar to the corresponding Chl fluorescence (cf. Fig. 2B). However, absolute intensities of the RLS main bands of bean thylakoids (Fig. 6B) were higher than appropriate bands in pea (Fig. 6A).

3.5. Proteins and lipids structure of thylakoid membranes in absence and presence of Mg^{2+} ions

Fig. 7 presents region of the infrared spectra normalized at 1650 cm^{-1} of pea and bean thylakoids incubated without (0 mM) (Fig. 7A, D) or with 6 mM $MgCl_2$ (Fig. 7B, E). The Amide I region (1700–1580 cm^{-1}) corresponds to peptide bond carbonyl group vibration [28], whereas the band between 1760 and 1710 cm^{-1} is related to ester C=O vibration, a bond present in lipids due to binding of fatty acid to the glycerol backbone [38]. Since the ester C=O group is not present in polypeptide chains, the ratio of integrated intensities of Amide I band to ester C=O vibration, informs about the relative proportion of proteins to lipids as was described for tobacco and *Synechocystis* thylakoids as well as for artificial membranes [38–40]. This ratio showed a lower relative protein/lipid proportion in pea than in bean thylakoids (Fig. 7C, F). However, both in pea and bean thylakoids the protein/lipid ratio was independent of $MgCl_2$ treatment (Fig. 7C, F).

Further relationship between lipid ordering in thylakoids under Mg^{2+} ions treatment was performed by analysis of IR region at 3000–2800 cm^{-1}, corresponding to deforming stretching vibrations of CH_2 and CH_3 groups of membrane lipid acyl chains. The spectrum could be fitted with six specific Gaussian components (not showed). Changes in disorder of fatty acyl chains correspond to the upshifted frequency of the symmetric stretching band of CH_2 groups ($\nu_{sym}CH_2$) at around 2850 cm^{-1} [38,39]. However, the maxima of the $\nu_{sym}CH_2$ band, estimated to 2851 ± 0.5 and 2850 ± 0.8 cm^{-1} in pea and bean thylakoids were unchaged in absence (0 mM) and in the presence of 6 mM $MgCl_2$ in samples (not showed). Furthermore, the band centered at 2830 cm^{-1} can be assigned to the symmetric C—H stretching vibrations of acyl chains of lipids in domains characterized by relatively low molecular motions, e.g. due to the interactions with proteins [38,39]. However, the ratio of total lipid region area to the C—H stretching band area did not change in the presence of 6 mM $MgCl_2$, both in pea and bean thylakoids (Fig. 7C, F). Thus, these results suggest that both structural lipid disorder and lipid–protein interaction were not affected by $MgCl_2$ presence.

Changes in protein structure were investigated by analysis of the individual Gaussian component in Amide I region (Fig. 7). Main band

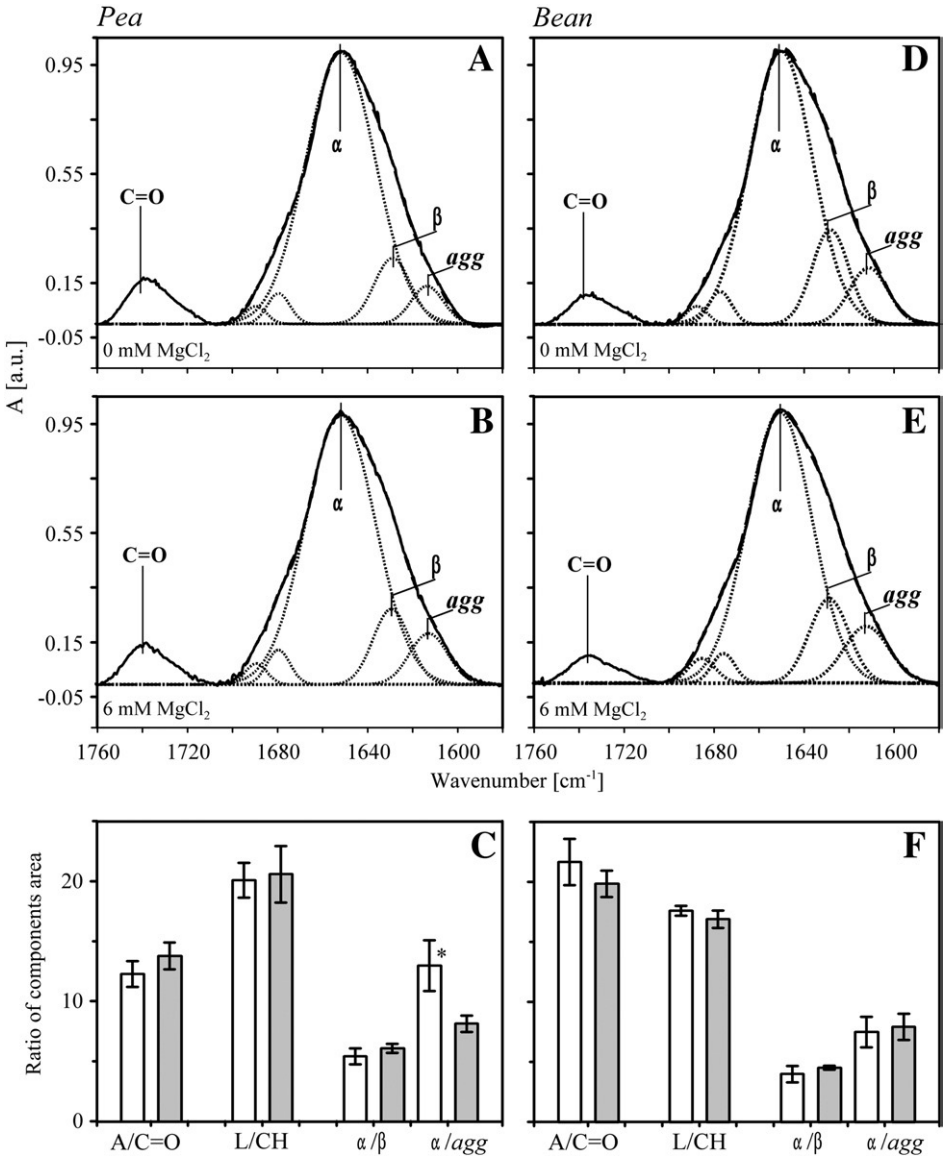

Fig. 7. Normalized (at 1650 cm^{-1} to one) infrared absorption spectra in the Amide I and ester C=O regions recorded from pea (panels A, B) and bean (panels D, E) thylakoids deposited from buffer without Mg^{2+} ions (panels A, D) and buffer containing 6 mM $MgCl_2$ (panels B, E). The original spectra (thin solid line), the deconvolution components (dotted lines) and fitted curves (dashed lines) are presented. Panels C and F show the ratio of the area beneath of spectral components for respective pea and bean spectra. A/C=O—ratio of Amide I to ester C=O; L/C-H—ratio of total CH_n groups vibration to low energy C—H vibration; α/β -ratio of α-structure to parallel β-structure; α/*agg*—ratio of α-structure to aggregates strands. Empty bar—spectra recorded in buffer without Mg^{2+} ions, grey bars—in buffer with 6 mM $MgCl_2$. The data are mean values ± SD from 4 independent experiments. $^{*}P<0.037$.

centered at around 1650 cm^{-1} corresponds to α-helical chains of membrane protein while bands centered at around 1680 and 1689 cm^{-1} were assigned to turn and loops, and antiparallel β-structures, respectively. The origin of bands at 1630 cm^{-1} is associated with the formation of hydrogen bonds between the carbonyl groups and the amino groups of residues of neighboring α-helices and formally designated as a parallel β-structure. The low-energy band at 1610 cm^{-1} is attributed to aggregates strands [28,33,41]. Furthermore, in the case of thylakoid membrane, the ratio of integrated intensities of α-helical band to the parallel β-structure (α/β) and to aggregates strands (α/*agg*) represent the aggregation level of thylakoid protein inside and outside membrane, respectively [33,41]. Comparison of such estimated ratio showed that in bean thylakoids incubated without $MgCl_2$, the relative proportion of α-helical (1650 cm^{-1}) to aggregated (1610 cm^{-1}) structures (Fig. 7F) is noticeably lower than in pea thylakoids (Fig. 7C). Furthermore, as shown in Fig. 7C in absence and in the presence of Mg^{2+} ions in pea thylakoids, the relative fraction of β-structure was unchanged, whereas a decrease of α/*agg* ratio was observed. In bean thylakoids these parameters were unchanged (Fig. 7F). Such results suggest that polypeptide fragments located outside the membrane bilayer contributed to the $MgCl_2$-induced formation of aggregated structures. This was observed in pea thylakoids only.

3.6. Magnesium ions effect on spatial distribution of Chl fluorescence in intact pea and bean chloroplasts

Images of intact pea chloroplasts revealed by CLSM showed that Mg^{2+} ions significantly affected chloroplasts structure. At low magnesium concentration (0 mM $MgCl_2$ in incubation buffer) Chl fluorescence exhibited wide dispersion within pea chloroplasts (Fig. 8A). It does not mean that all membranes containing LHCII–PSII supercomplexes and LHCII trimers were unfolded. Fig. 8A clearly indicated that there were small and irregularly distributed appressed regions inside intact

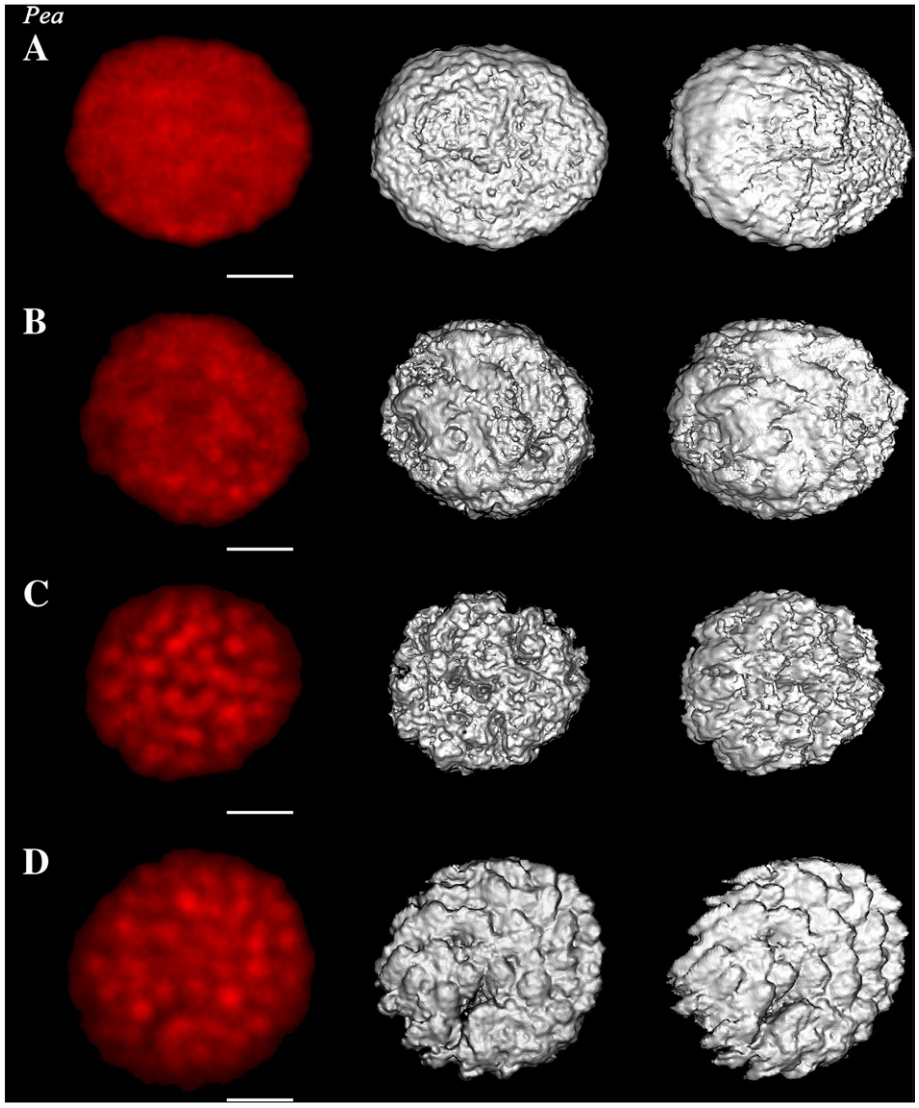

Fig. 8. Effect of $MgCl_2$ concentration on pea intact chloroplast structure revealed by CLSM images and 3D reconstruction. Before embedded on polylysine layer, isolated intact chloroplasts were incubated without $MgCl_2$ (A), or with medium containing $MgCl_2$ in 0.5 mM (B), 4 mM (C) and 6 mM (D) concentrations. The red images present the middle cross-section of deconvolved stack of CLSM images. Grey images represent 3D models of intact pea and bean chloroplasts created after deconvolution. Each time face and side view of 3D chloroplast models is shown. Bar = 2 μm. Each image is representative for at least 10 independent experiments.

chloroplasts. Slight addition (0.5 mM) of $MgCl_2$ led to certain condensation of Chl fluorescence into brightly red fluorescent discs, but fluorescence dispersion was also observed (Fig. 8B). Addition of 4 mM $MgCl_2$ to the incubation buffer resulted in big and well-distinguished fluorescent areas formation (Fig. 8C). 6 mM magnesium ion concentration caused subsequent fluorescence condensation; brightly red areas were clearly separated by dark space (Fig. 8D).

We created 3D structures based on 87–104 fluorescence images from different focal depths, where spatial layout of Chl fluorescence was shown. Computerized 3D images of intact pea chloroplasts incubated at different ion concentrations highlighted the tendency observed directly by CLSM. 3D model shows a slightly wrinkled sphere if the incubation buffer contained no Mg^{2+} ions (Fig. 8A). It might suggest, that in unstacking conditions, grana stacks were unfolded and merged with the neighboring stroma thylakoids. Consequently, thylakoid membranes form continuous surface within chloroplast and LHCII/PSII complexes were evenly distributed around the membranes (Fig. 8A). The next 3D models show (Fig. 8B–D) that the subsequent gradual magnesium addition led to an increase of surface irregularity. Spatial layout of Chl fluorescence forms distinguished, sharply outlined spatial areas with diameter of about 400 nm, which in the presence of 6 mM $MgCl_2$ occupied majority of the organellum volume (Fig. 8D). $MgCl_2$-induced successive spatial condensation of Chl fluorescence suggests that unfolded, unstacked membranes (Fig. 8A) were transformed into many stacked areas (Fig. 8D). Furthermore, changes of spatial visualization of Chl fluorescence under increasing ionic force might be related to the accumulation of LHCII/PSII in grana and at least partial separation of PSI/PSII complexes between the stroma and grana thylakoids (cf. Fig. 3A–D).

Images revealed by CLSM exhibited minor influence of magnesium ions on the structure of intact bean chloroplasts (Fig. 9). At low $MgCl_2$ concentration (0 mM $MgCl_2$ in incubation buffer), in bean chloroplasts (Fig. 9A), in contrast to pea (Fig. 8A), many tiny, but distinct fluorescent areas of Chl fluorescence were observed. Gradual addition of $MgCl_2$ to the incubation buffer caused formation of bigger and better distinguished bright fluorescence regions. Moreover, bigger non-fluorescence dark spaces between red regions emerged (Fig. 9B–D). However, even in the presence of 6 mM $MgCl_2$, red fluorescence regions inside bean chloroplasts were less regular and smaller (Fig. 9D) in comparison with bigger fluorescence spots observed in pea chloroplasts (cf. Fig. 8D).

3D images of bean chloroplasts, obtained on the base of stack of optical slices, confirmed different effect of magnesium ions on the

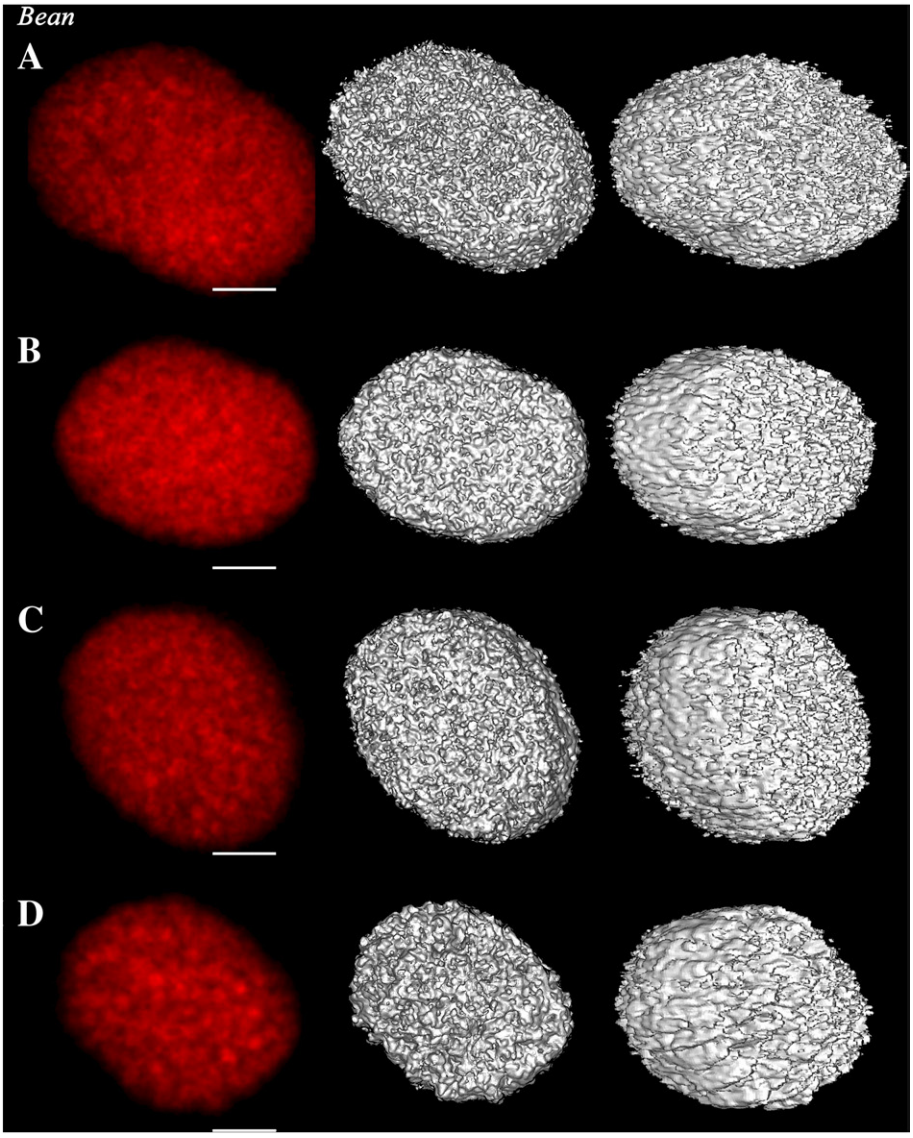

Fig. 9. Effect of $MgCl_2$ concentration on bean intact chloroplast structure revealed by CLSM images and 3D reconstruction. Before embedded on polylysine layer isolated intact chloroplasts were incubated without $MgCl_2$ (A), or with medium containing $MgCl_2$ in 0.5 mM (B), 4 mM (C) and 6 mM (D) concentrations. Description as in the legend to Fig. 8.

chloroplast structure of the two examined species. In case of incubation without Mg^{2+} cations the model shows a finely and densely folding surface of membranes within bean chloroplasts (Fig. 9A). This might suggest that under those conditions LHCII/PSII complexes were arranged in many separated regions and did not migrate to other parts of thylakoids (cf. Fig. 3E–H). If these smaller fluorescence regions in bean chloroplasts were related to stacked thylakoids depletion of $MgCl_2$ from incubation buffer would not cause massive unfolding of membranes. Subsequent increase of $MgCl_2$ concentration led to increase of size and decrease of the number of 3D areas inside bean chloroplasts (Fig. 9B–D). This means, that increase of the stacking membrane degree might be caused by merging of smaller stacked regions. However, this stacking process in bean chloroplast was subtle (Fig. 9D) as compared with changes observed within pea chloroplasts (Fig. 8D).

4. Discussion

Commonly accepted models of thylakoid stacking assume two simultaneous processes, (i) vertical appression of adjacent membranes and (ii) lateral separation of CP complexes [20,42]. These phenomena can be explained by an increase of the van der Waals attraction and decrease of electrostatic and hydration repulsion between neighbouring membranes [42]. Thus, the presence of cations, e.g. Mg^{2+} ions, seems to be responsible for enhanced electrostatic screening of negative surface charges of thylakoid membranes. In stacked grana membranes dominate the intramembrane ordered LHCII–PSII supercomplexes (PSIIα) [18], while molecular architecture of PSI with protrusion at the stroma-facing surface prevents its migration to the thylakoid partition gap [17], what explains the lateral separation of CP complexes.

We have found two plant species of which chloroplast structures undergo different alterations under magnesium ion treatment. We will now address the key question what is the reason of such remodelling. Pea chloroplasts contain large stacked areas, while, fewer distinguished appressed regions are observed in bean chloroplasts (Fig. 1), probably as a consequence of different organization of CP complexes [9,10,43]. The relative LHCI–PSI/LHCII–PSII fluorescence ratio is higher in bean thylakoids [25] suggesting lower abundance of PSIIα in bean than in pea thylakoids. Because the ordering of LHCII–PSII supercomplexes is an essential component of stacked grana [18 and references therein], smaller size of appressed regions in bean thylakoids may be directly

related to smaller amounts of PSIIα. Similarly, the lower PSI/PSII fluorescence ratio in pea thylakoids [25] should be correlated with large grana areas in pea chloroplasts (Figs. 1, 8C).

The analysis of the Gaussian component of the infrared spectrum shows that the protein/lipid ratio is higher in bean than in pea thylakoids (Fig. 7), thus the average protein density is higher in bean [38–40]. Since about 60% of total lipids contribute to the boundary lipids [44] and the protein/lipid ratio in bean is 1.5 higher than in pea lower amount of bulk lipid phase is present in bean thylakoids. Probably it might influence different arrangement of appressed and non-appressed thylakoid membranes in pea and bean chloroplasts (Figs. 8, 9).

Biochemical and ultrastructural data analysis indicates that protein–protein interactions might play an important role for short-range protein organization and the stacking of grana discs, especially by formation of the LHCII–PSII supercomplexes (PSIIα) and slightly larger assembly megacomplexes [18]. However, at high protein density this effect becomes less important than in isolated grana membranes, where proteins occupy about 80% of grana space and low salt treatment does not change functional interactions between LHCII and PSII [22]. Recent investigation showed that approximately 75% of the protein complexes in isolated grana thylakoids were almost immobile, but 25% moved relatively fast [45]. The diffusion coefficient in crowded membranes is distance-dependent, i.e. the diffusion time is longer in larger grana discs. Thus, molecular crowding in large grana might prevent lateral diffusion of LHCII/PSII [18] and should lead to a decrease in sensitivity to Mg^{2+} ion treatment. However in our experimental conditions the $MgCl_2$-dependent large-scale stacking phenomenon is observed only under formation of large stacked areas occuring in pea chloroplasts, while structures of small appressed regions in bean chloroplast slightly depend on cation concentration (Figs. 8, 9).

We postulate that a kind of "spatial encumbrance" exists in bean chloroplasts, that is caused by a different megacomplexes/microdomains arrangement. We showed by 120 K fluorescence (Fig. 3E–F) [25] and mild-denaturing electrophoresis [9,10] that the amount of LHCI–PSI is larger than LHCII–PSII. Therefore LHCI–PSI might be an essential component of these microdomains. These domains should be localized outside the appressed membranes because PSI protrusion prevents migration of this complex to grana. Therefore, the influence of magnesium ions on the overall bean chloroplast structure is limited (Fig. 9). In pea thylakoids under increasing magnesium ion concentration we observed similar effects as described for spinach [22] and *Arabidopsis thaliana* [16]. In this case larger area of stroma thylakoids could be distinguished (Fig. 1, 8) with lower amounts of LHCI–PSI complexes (Fig. 3) [9,10]. Such membrane arrangement might enable randomization of CP complexes and unstacking of grana in the absence of Mg^{2+} ions (Fig. 8A) or segregation and grana formation in the $MgCl_2$ presence (Fig. 8D).

The freeze-fracture electron microscopy of unstacked spinach grana showed disorder of the LHCII–PSIIα megacomplexes, but not complete disassembly of PSIIα supercomplexes. On the other hand, the Mg^{2+} ions induced restacking of thylakoids caused formation of ordered LHCII–PSIIα microdomains [21]. On that basis Kirchhoff et al. [21] proposed that the protein arrangement in grana thylakoids is a self-organized process related to specific interaction of LHCII–trimer with PSII dimers and with lipids surrounding the membrane proteins. Thus, the hydrophobic recognition might be the main mechanism in lateral interaction between CP complexes [21]. We showed that $MgCl_2$-induced membrane stacking does not change the fraction of boundary lipids and aggregation level of thylakoid proteins inside the membrane (Fig. 7C, F). Thus our data confirmed earlier suggestions [44] that changes in weak associations between supercomplexes is created by boundary lipids without formation of direct protein–protein bonds.

On the other hand, stacking of adjacent membranes is correlated with charge distribution on the stromal face of LHCII trimers and PSII subunits, which may be balanced by presence of Mg^{2+} ions [16]. Decrease of electrostatic repulsions enables direct interaction between proteins in opposite membranes, as is shown by analysis of individual Gaussian components in Amide I region (Fig. 7). $MgCl_2$ enhances the level of the aggregate strands, which suggests formation of hydrogen bonds between polypeptide fragments located outside the membrane bilayer, i.e. probably between hydrophilic N-terminal domain of LHCII localized on the stroma surface of thylakoids [46].

Furthermore, changes in charge of outer-membrane parts of proteins might be involved in the lateral arrangements of LHCII–PSII complexes [21], probably by formation of protein bridges above the lipid bilayers [44 and references therein]. It is likely that both cation-dependent lateral movement of proteins and vertical thylakoids stacking occur simultaneously and depend on each other [21], but is also related to cation concentration [23]. This statement corresponds to our observation, that nearly maximal Chl fluorescence is observed at lower $MgCl_2$ (Fig. 2), whereas thylakoids stacking takes place at higher Mg^{2+} ions concentrations (Fig. 8, 9). Due to observations with atomic force microscopy [22] the lateral distance between Chls in different LHCII complexes in appressed membranes is calculated to be about 2 nm, which is sufficient for efficient transfer of excitonic energy. The minimal vertical distance between Chl molecules in LHCII complexes localized in adjacent membrane is larger, around 5.5 nm [22]. This calculation supports the lateral energy transfer and indicates, that the thylakoid stacking is not strictly related to the excitonic connectivity of PSIIα [22,23].

The main aim of our research was CLSM observation and 3D computer modelling of the whole chloroplasts in nearly intact state (*in situ*) (Figs. 8, 9). We showed that magnesium ions induced massive reorganization of the entire chloroplast space, not only by formation of appressed regions, but also by significant change of non-appressed areas (Fig. 8). All our 3D visualizations are in agreement with spectroscopic data, e.g. the level of RLS (Fig. 6) and numbers of appressed areas (Figs. 8, 9) and extend analysis of stacking process. Especially in pea chloroplasts, we can directly observe successive stages of appressed membranes formation from uniform continuous surface (Fig. 8A) to many distinguished stacked areas (Fig. 8C, D). Since the stack of two adjacent thylakoid membranes is about 17 nm height [47], the stacked regions in our models of pea chloroplasts with a diameter about 400 nm (Fig. 8C, D) should be composed from at least 20 membrane pairs. Otherwise, on the wrinkled surface of unstacked membranes our models revealed three or four times smaller appressed regions (Fig. 8A, B) suggesting that these areas consist of fewer paired membranes. Models of bean chloroplast present similar but less pronounced tendencies towards formation of appressed regions, from tiny areas (Fig. 9A) to about twice as large, distinctive regions (Fig. 9D). Thus, probably there are fewer paired membranes in bean stacks than in pea. Moreover, under transformation from unstacking to stacking conditions both type of chloroplast revealed noticeable decrease of the total surface area (Figs. 8A, 9A versus Figs. 8D, 9D), suggesting coordinated refolding of entire membranes within chloroplasts. Due to low optical resolution of CLSM we could not create appropriate topological model for stacking process. Mostly because higher resolution microscopic methods [8,13] did not give unambiguous conclusions. However, our models clearly indicated that the stacking process concerns simultaneously all membranes within chloroplast. Thus, spatial structures of the whole chloroplast represent the thermodynamic optimum in definite environmental condition [16].

In summary, comparison of thylakoids stacking phenomena of pea and bean chloroplasts by complementary methods can lead to general conclusions and extend recent understanding of this process. We have shown that protein/lipid ratio and arrangement of supercomplexes influence formation of appressed membranes. We suggest that not only the size differences between PSII–LHCII and PSI–LHCI, but also

the quantitative and/or qualitative composition of microdomains is an important factor in lateral segregation of photosystems. Moreover, stacking processes always affect the structural changes of chloroplast as a whole.

Acknowledgments

This work is supported by Polish Ministry of Science and Higher Education Grant No N303 4185 33.

References

[1] J.P. Dekker, E.J. Boekema, Supramolecular organization of thylakoid membrane proteins in green plants, Biochim. Biophys. Acta 1706 (2005) 12–39.
[2] H. Kirchhoff, I. Tremmel, W. Haase, U. Kubitscheck, Supramolecular Photosystem II organization in grana thylakoid membranes: evidence for a structured arrangement, Biochemistry 43 (2004) 9204–9213.
[3] J. Nield, J. Barber, Refinement of the structural model for the Photosystem II supercomplex of higher plants, Biochim. Biophys. Acta 1757 (2006) 353–361.
[4] R. Danielsson, M. Suorsa, V. Paakkarinen, P.-Å. Albertsson, S. Styring, E.-M. Aro, F. Mamedov, Dimeric and Monomeric Organization of Photosystem II. Distribution of five distinct complexes in the different domains of the thylakoid membrane, J. Biol. Chem. 281 (2006) 14241–14249.
[5] F. Mamedov, R. Danielsson, R. Gadjieva, P.-Å. Albertsson, S. Styring, E.P.R. characterization of photosystem II from different domains of the thylakoid membrane, Biochemistry 47 (2008) 3883–3891.
[6] F. Klimmek, U. Ganeteg, J.A. Ihalainen, H. van Roon, P.E. Jensen, H.V. Scheller, J.P. Dekker, S. Jansson, Structure of the higher plant light harvesting complex I: in vivo characterization and structural interdependence of the Lhca proteins, Biochemistry 44 (2005) 3065–3073.
[7] R. Kouřil, A. Zygadlo, A.A. Arteni, C.D. de Wit, J.P. Dekker, P.E. Jensen, H.V. Scheller, E.J. Boekema, Structural characterization of a complex of photosystem I and light-harvesting complex II of *Arabidopsis thaliana*, Biochemistry 44 (2005) 10935–10940.
[8] S.G. Chuartzman, R. Nevo, E. Shimoni, D. Charuvi, V. Kiss, I. Ohad, V. Brumenfeld, Z. Reich, Thylakoid membrane remodeling during state transitions in *Arabidopsis*, Plant Cell 20 (2008) 1029–1039.
[9] M. Garstka, A. Drożak, M. Rosiak, J.H. Venema, B. Kierdaszuk, E. Simeonova, P.R. van Hasselt, J. Dobrucki, A. Mostowska, Light-dependent reversal of dark-chilling induced changes in chloroplast structure and arrangement of chlorophyll–protein complexes in bean thylakoid membranes, Biochim. Biophys. Acta 1710 (2005) 13–23.
[10] M. Garstka, J.H. Venema, I. Rumak, K. Gieczewska, M. Rosiak, J. Kozioł-Lipińska, B. Kierdaszuk, W.J. Vredenberg, A. Mostowska, Contrasting effect of dark-chilling on chloroplast structure and arrangement of chlorophyll–protein complexes in pea and tomato—plants with a different susceptibility to non-freezing temperature, Planta 226 (2007) 1165–1181.
[11] P.O. Arvidsson, C. Sundby, A model for the topology of the chloroplast thylakoid membrane, Aust. J. Plant Physiol. 26 (1999) 687–694.
[12] L. Mustárdy, G. Garab, Granum revisited. A three-dimensional model—where things fall into place, Trends Plant Sci. 8 (2003) 117–122.
[13] L. Mustárdy, K. Buttle, G. Steinbach, G. Garab, The three-dimensional network of the thylakoid membranes in plants: quasihelical model of the granum-stroma assembly, Plant Cell 20 (2008) 2552–2557.
[14] E. Shimoni, O. Rav-Hon, I. Ohad, V. Brumfeld, Z. Reich, Three-dimensional organization of higher-plant chloroplast thylakoid membranes revealed by electron tomography, Plant Cell 17 (2005) 2580–2586.
[15] V. Brumfeld, D. Charuvi, R.H. Smith, A note on three-dimensional models of higher-plant thylakoid networks, Plant Cell 20 (2008) 2546–2551.
[16] E.-H. Kim, W.S. Chow, P. Horton, J.M. Anderson, Entropy-assisted stacking of thylakoid membranes, Biochim. Biophys. Acta 1708 (2005) 187–195.
[17] A. Borodich, I. Rojdestvenski, M. Cottam, G. Öquist, Segregation of the photosystems in thylakoids depends on their size, Biochim. Biophys. Acta 1606 (2003) 73–82.
[18] H. Kirchhoff, Molecular crowding and order in photosynthetic membranes, Trends Plant Sci. 13 (2008) 201–207.
[19] R. Danielsson, P.-Å. Albertsson, F. Mamedov, S. Styring, Quantifications of photosystem I and II in different parts of the thylakoid membrane from spinach, Biochim. Biophys. Acta 1608 (2004) 53–61.
[20] G. Garab, L. Mustárdy, Role of LHC II-containing macrodomains in the structure, function and dynamics of grana, Aust. J. Plant Physiol. 26 (1999) 649–658.
[21] H. Kirchhoff, W. Haase, S. Haferkamp, T. Schott, M. Borinski, U. Kubitscheck, M. Rögner, Structural and functional self-organization of Photosystem II in grana thylakoids, Biochim. Biophys. Acta 1767 (2007) 1180–1188.
[22] H. Kirchhoff, M. Borinski, S. Lenhert, L. Chi, C. Büchel, Transversal and lateral exciton energy transfer in grana thylakoids of spinach, Biochemistry 43 (2004) 14508–14516.
[23] K. Stoitchkova, M. Busheva, E. Apostolova, A. Andreeva, Changes in the energy distribution in mutant thylakoid membranes of pea with modified pigment content. II. Changes due to magnesium ions concentration, J. Photochem. Photobiol. B: Biology 83 (2006) 11–20.
[24] D. Kaftan, V. Brumfeld, R. Nevo, A. Scherz, Z. Reich, From chloroplasts to photosystems: in situ scanning force microscopy on intact thylakoid membranes, EMBO J. 21 (2002) 6146–6153.
[25] I. Rumak, K. Gieczewska, J. Kozioł-Lipińska, B. Kierdaszuk, A. Mostowska, M. Garstka, Arrangement of chlorophyll–protein complexes determines chloroplast structure, in: J.F. Allen, E. Gantt, J.H. Golbeck, B. Osmond (Eds.), Photosynthesis. Energy from the Sun, Springer, Dordrecht, 2008, pp. 791–793.
[26] M.F. Hipkins, N.R. Baker, Photosynthesis energy transduction, a practical approach, IRL Press, Oxford, Practical Approach Series, 1986.
[27] A. Andreeva, K. Stoitchkova, M. Busheva, E. Apostolova, Changes in the energy distribution between chlorophyll–protein complexes of thylakoid membranes from pea mutants with modified pigment content. I. Changes due to the modified pigment content, J. Photochem. Photobiol. B. 70 (2003) 153–162.
[28] L.K. Tamm, S.A. Tatulian, Infrared spectroscopy of proteins and peptides in lipid bilayers, Q. Rev. Biophys. 30 (1997) 365–429.
[29] M. Mehta, V. Sarafis, C. Critchley, Thylakoid membrane architecture, Austr. J. Plant Physiol. 26 (1999) 709–716.
[30] J.M. Anderson, E.-M. Aro, Grana stacking of Photosystem II in thylakoid membranes of higher plant leaves under sustained high irradiance: a hypothesis, Photosynth. Res. 41 (1994) 315–326.
[31] A.V. Ruban, J.P. Dekker, P. Horton, R. van Grondelle, Temperature dependence of the chlorophyll fluorescence from light harvesting complex II of higher plants, Photochem Photobiol 61 (1995) 216–221.
[32] A. Jajoo, S. Bharti, Govindjee, Inorganic anions induce state changes in spinach thylakoid membranes, FEBS Lett. 434 (1998) 193–196.
[33] W.I. Gruszecki, W. Grudzinski, M. Gospodarek, M. Patyra, W. Maksymiec, Xanthophyll-induced aggregation of LHCII as a switch between light-harvesting and energy dissipation systems, Biochim. Biophys. Acta 1757 (2006) 1504–1511.
[34] A.V. Ruban, F. Calkoen, S.L.S. Kwa, R. van Grondelle, P. Horton, J.P. Dekker, Characterisation of LHCII in the aggregated state by linear and circular dichroism spectroscopy, Biochim Biophys Acta 1932 (1997) 61–70.
[35] M. Garstka, A. Jagielski, Peroxidative reactions attenuate oxygen effect on spectroscopic properties of isolated chloroplasts, J. Photochem. Photobiol. B. 64 (2001) 82–92.
[36] H. Kirchhoff, H.-J. Hinz, J. Rösgen, Aggregation and fluorescence quenching of chlorophyll a of the light-harvesting complex II from spinach in vitro, Biochim. Biophys. Acta 1606 (2003) 105–116.
[37] A. Ventrella, L. Catucci, G. Mascolo, A. Corcelli, A. Agostiano, Isolation and characterization of lipids strictly associated to PSII complexes: Focus on cardiolipin structural and functional role, Biochim. Biophys. Acta 1768 (2007) 1620–1627.
[38] B. Szalontai, Z. Kóta, H. Nonaka, N. Murata, Structural consequences of genetically engineered saturation of the fatty acids of phosphatidylglycerol in tobacco thylakoid membranes, An FTIR study, Biochemistry 42 (2003) 4292–4299.
[39] B. Szalontai, Y. Nishiyama, Z. Gombos, N. Murata, Membrane dynamics as seen by Fourier transform infrared spectroscopy in a cyanobacterium, Synechocystis PCC 6803. The effects of lipid unsaturation and the protein-to-lipid ratio, Biochim. Biophys. Acta 1509 (2000) 409–419.
[40] E. Goormaghtigh, V. Raussens, J.M. Ruysschaert, Attenuated total reflection infrared spectroscopy of proteins and lipids in biological membranes, Biochim. Biophys. Acta 1422 (1999) 105–185.
[41] W.I. Gruszecki, M. Gospodarek, W. Grudziński, R. Mazur, K. Gieczewska, M. Garstka, Light-induced change of configuration of the LHCII-bound xanthophyll (tentatively assigned to violaxanthin): a resonance Raman study, J. Phys. Chem. B. 113 (2009) 2506–2512.
[42] J. Barber, W.S. Chow, A mechanism for controlling the stacking and unstacking of chloroplast thylakoid membranes, FEBS Lett. 105 (1979) 5–10.
[43] I. Rumak, K. Gieczewska, B. Kierdaszuk, A. Mostowska, W.I. Gruszecki, M. Garstka, in: J.F. Allen, E. Gantt, J.H. Golbeck, B. Osmond (Eds.), 3D chloroplast structure, in: Photosynthesis. Energy from the Sun, Springer, Dordrecht, 2008, pp. 771–774.
[44] H. Kirchhoff, U. Mukherjee, H.-J. Galla, Molecular architecture of the thylakoid membrane: lipid diffusion space for plastoquinone, Biochemistry 41 (2002) 4872–4882.
[45] H. Kirchhoff, S. Haferkamp, J.F. Allen, D.B.A. Epstein, C.W. Mullineaux, Protein diffusion and macromolecular crowding in thylakoid membranes, Plant Physiol. 146 (2008) 1571–1578.
[46] Z. Liu, H. Yan, K. Wang, T. Kuang, J. Zhang, L. Gui, X. An, W. Chang, Crystal structure of spinach light-harvesting complex at 2.72 Å resolution, Nature 428 (2004) 287–292.
[47] H. Kirchhoff, S. Lenhert, C. Büchel, L. Chi, J. Nield, Probing the organization of photosystem II in photosynthetic membranes by atomic force microscopy, Biochemistry 47 (2008) 431–440.